Available online at www.sciencedirect.com
ScienceDirect
Journal of Solid State Chemistry 181 (2008) 1–6
JOURNAL OF SOLID STATE CHEMISTRY
www.elsevier.com/locate/jssc

Synthesis, crystal structure, and physical properties of the monoclinic form of the $R_4Mo_4O_{11}$ compounds (R = Yb and Lu) containing infinite chains of trans-edge-shared octahedral clusters

Philippe Gall[b], Patrick Gougeon[a,*]

[a]*Laboratoire de Chimie du Solide et Inorganique Moléculaire, UMR CNRS 6226, Université de Rennes 1, Avenue du Général Leclerc, 35042 Rennes-Cedex, France*
[b]*Laboratoire de Chimie des Materiaux Inorganiques et de Cristallographie, 20 avenue des buttes de Coesmes, 35043 Rennes cedex, France*

Received 31 August 2007; received in revised form 15 October 2007; accepted 16 October 2007
Available online 3 December 2007

Abstract

Polycrystalline samples and single crystals of the $R_4Mo_4O_{11}$ compounds (R = Yb and Lu) were synthesized by solid-state reactions at high temperature in sealed Mo crucibles. The structure of $Lu_4Mo_4O_{11}$ ($a = 10.5611(1)$, $b = 5.61930(5)$, $c = 15.6877(2)$, $\beta = 99.5131(4)$ and $Z = 4$) was determined by single crystal X-ray diffraction and refined by least squares on F^2 converging to $R_1 = 0.0425$, $wR_2 = 0.0980$ for 3508 intensities. Contrary to the $R_4Mo_4O_{11}$ compounds with lighter rare earths, which crystallize in the orthorhombic space group *Pbam*, the Yb and Lu compounds crystallize in the monoclinic space group $P2/m$. The $R_4Mo_4O_{11}$ compounds contain distorted infinite oxide-molybdenum chains of trans-edge-sharing Mo_6 octahedra diluted with the rare earths. Magnetic susceptibility measurements indicate that the oxidation state of the Yb atoms is +3, affording 14 metallic valence electrons per Mo_4 fragment and, the absence of localized moments on the Mo network. Resistivity measurements on single crystals show that the $Yb_4Mo_4O_{11}$ and $Lu_4Mo_4O_{11}$ compounds are small band-gap semi-conductors.

Keywords: Reduced molybdenum oxides; Molybdenum chains; Rare earths; Magnetic susceptibility; Resistivity measurement

1. Introduction

Since the discovery of infinite chains of trans-edge-sharing Mo_6 octahedra in $NaMo_4O_6$ by Torardi and McCarley [1], four other crystallographic structure types containing similar molybdenum chains have been discovered: $Sc_{0.75}Zn_{1.25}Mo_4O_7$ [2], $Mn_{1.5}Mo_8O_{11}$ [3], MMo_8O_{10} (M = Li, Zn) [4], and $R_4Mo_4O_{11}$ (R = Nd–Tm) [5,6]. The crystal structures of these compounds differ from each other in the manner in which the infinite molybdenum octahedral chains are coupled together through the oxygen atoms to form the three-dimensional lattices. Another important difference between the trans-edge-sharing Mo_6 octahedral chains present in the above different structure types are the number of electrons available for Mo–Mo bonding, often called metal cluster electrons (MCE). The MCE on which greatly depend the physical properties in these materials may vary from 13 electrons per Mo_4 repeat unit in the MMo_4O_6 (M = Na, K, and In) compounds to 15 in $ZnMo_8O_{10}$. The MCE also governs the geometry of the chains. Indeed, while they are regular in the MMo_4O_6 (M = Na, K, and In) [7] compounds with 13 electrons per Mo_4 repeat unit, they distort for MCEs greater than 13 as observed in $Sc_{0.75}Zn_{1.25}Mo_4O_7$ and $Ho_4Mo_4O_{11}$. In point of fact, EHT calculations performed by Hughbanks and Hoffmann on $NaMo_4O_6$ [8] allowed them to show that systems with electron count greater than 13 MCE per Mo_4 repeat unit should distort because of the occupation of antibonding bands.

Recently, we have investigated the crystal and electronic structures as well as the physical properties of the orthorhombic compounds $R_4Mo_4O_{11}$ (R = Sm, Gd, Tb, Dy, Ho, Er, Tm, and Y) [6]. The latter compounds with 14

*Corresponding author. Fax: +33 2 23 23 67 99.
E-mail address: patrick.gougeon@univ-rennes1.fr (P. Gougeon).

0022-4596/$ - see front matter © 2007 Elsevier Inc. All rights reserved.
doi:10.1016/j.jssc.2007.10.024

electrons per Mo_4 repeat are small band-gap semiconductors and magnetic susceptibility studies are in agreement with the presence of R^{3+} ions. In addition, antiferromagnetic orderings have also been observed for the $R_4Mo_4O_{11}$ compounds with R = Gd to Tm below 5 K. In this paper, we report on the synthesis, the crystal structure, the temperature dependences of the electrical resistivity and magnetic susceptibility of the related monoclinic compounds $Yb_4Mo_4O_{11}$ and $Lu_4Mo_4O_{11}$.

2. Experimental section

2.1. Synthesis and crystal growth

X-ray diffractometrically pure powders of $Yb_4Mo_4O_{11}$ and $Lu_4Mo_4O_{11}$ were prepared from stoichiometric mixtures of MoO_3 (Strem Chemicals, 99.9%), Mo (Cime bocuze, 99.9%) and R_2O_3 (Rhône Progil S.A, 99.999%). Before use the Mo powder was heated under a hydrogen flow at 1000 °C for 6 h and the rare-earth oxides were prefired at 800 °C overnight and left at 600 °C before weighing them. The mixtures were pressed into pellets (ca. 5 g) and loaded into molybdenum crucibles which were previously outgassed at about 1500 °C for 15 min under a dynamic vacuum of about 10^{-5} Torr. The Mo crucibles were subsequently sealed under a low argon pressure using an arc-welding system. The samples were heated at a rate of 300 °C/h to 1400 °C, kept at the temperature for 48 h and then cooled at 100 °C/h down to 1100 °C at which point the furnace was shut down and allowed to cool to room temperature. Both products were found to be single phase on the basis of their X-ray powder diffraction pattern carried out on an Inel position sensitive detector with a 0–120° 2θ aperture and Cu$K\alpha_1$ radiation (Fig. 1). Crystals were grown by heating stoichiometric mixtures of rare-earth oxides, molybdenum trioxide and molybdenum, all in powder form, with 5% (w/w) of K_2MoO_4 to assist the crystallization, in a sealed molybdenum crucible at about 1700 °C for 48 h. The crucible was then cooled at a rate of 100 °C/h down to 1000 °C, and finally furnace cooled to room temperature. Crystals thus obtained have the shape of needles with rectangular cross-section. Qualitative microanalyses using a JEOL JSM-35 CF scanning electron microscope equipped with a Tracor energy-dispersive-type X-ray spectrometer did not reveal the presence of potassium in the crystals. The absence of potassium was also confirmed by the single crystal structure determination by refining the site occupation factors of the rare earths. We have summarized in Table 1 the lattice parameters of the $Yb_4Mo_4O_{11}$ and $Lu_4Mo_4O_{11}$ compounds. Both compounds crystallize in the monoclinic $P2/m$ space group with four formula units per unit cell.

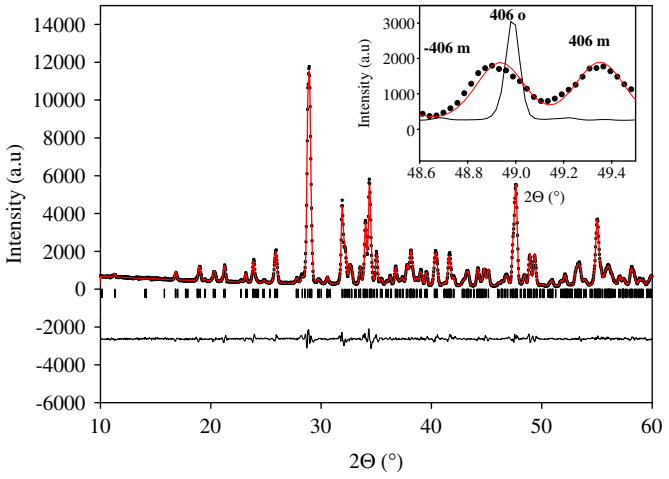

Fig. 1. Observed (dotted line), calculated (red line) and difference profiles for the refinement of $Yb_4Mo_4O_{11}$ in profile-matching mode (λ = 1.5406 Å).

2.2. Single crystal X-ray diffraction study of $Lu_4Mo_4O_{11}$

Several crystals of $Yb_4Mo_4O_{11}$ and $Lu_4Mo_4O_{11}$ were tested on a Nonius Kappa CCD diffractometer using graphite-monochromated Mo$K\alpha$ radiation (λ = 0.71073 Å). All of them present a substantial mosaic spread and were twinned. However, in all cases, all the reflections could be indexed in a monoclinic unit cell. The correspondence between the two crystalline components can be described either from a (100) symmetry plane or from a [001] twofold axis. The intensity data were collected on a single crystal of $Lu_4Mo_4O_{11}$ in the shape of a needle with dimensions $0.132 \times 0.040 \times 0.035\,mm^3$. The COLLECT program package [9] was used to establish the angular scan conditions (φ and ω scans) used in the data collection. The data set was processed with EvalCCD [10] for the integration procedure. An absorption correction was applied using the description of the crystal faces and the analytical method described by de Meulenaar and Tompa [11]. The structure was solved with the direct methods program SIR97 [12] and refined using SHELXL97 [13]. Crystallographic data and X-ray structural analysis for the $Lu_4Mo_4O_{11}$ compound are summarized in Table 2, and selected interatomic distances are listed in Table 3. Further details of the crystal structure investigation can be obtained from the Fachinformationszentrum Karlsruhe, 76344 Eggenstein-Leopoldshafen, Germany (fax: +49 7247 808 666; e-mail: crysdata@fiz.karlsruhe.de) on quoting the depository number CSD-418644.

Table 1
Unit cell parameters for the monoclinic $R_4Mo_4O_{11}$ compounds

	$Yb_4Mo_4O_{11}$	$Lu_4Mo_4O_{11}$
a (Å)	10.5866(2)	10.5611(1)
b (Å)	5.6269(1)	5.61930(5)
c (Å)	15.7255(3)	15.6877(2)
β (deg)	90.3804(7)	90.5131(4)
V (Å^3)	936.74(3)	930.965(17)

Table 2
Crystal data and structure refinements of $Lu_4Mo_4O_{11}$

Empirical formula	$Lu_4Mo_4O_{11}$
Formula weight (g/mol)	1259.64
Crystal system, space group	Monoclinic, $P2/m$
Unit cell dimensions (Å, deg)	$a = 10.5611(1)$ $b = 5.61930(5)$ $c = 15.6877(2)$ $\beta = 90.5131(4)$
Volume (Å^3)	930.965 (17)
Z, calculated density (g/cm^3)	4, 8.987
Absorption coefficient (mm^{-1})	47.244
Crystal color and habit	Black, needle like
Crystal size (mm^3)	$0.132 \times 0.040 \times 0.035$
Theta range for data collection (deg)	2.91–31.97
Limiting indices	$0 \leqslant h \leqslant 15$, $0 \leqslant k \leqslant 8$, $-23 \leqslant l \leqslant 23$
Reflections collected/unique	6150/3508
R (int)	0.0386
Absorption correction	Analytical
Max./min. transmission	0.2506/0.0627
Data/restraints/parameters	3508/0/145
Goodness-of-fit on F^2	1.081
R indices $[I>2\sigma(I)]$[a]	$R1 = 0.0425$, w$R2 = 0.0980$
Extinction coefficient	0.00027(5)
Largest diff. peak and hole (e/Å)	5.157 and –4.128

Table 3
Selected interatomic distances for $Lu_4Mo_4O_{11}$

Mo1 Mo1 2.571(3)	Mo1′ Mo1′ 2.574(3)
Mo1 Mo2 2.738(2)	Mo1′ Mo2′ 2.730(2)
Mo1 Mo2 2.766(2)	Mo1′ Mo2′ 2.735(2)
Mo1 Mo3 2.797(2)	Mo1′ Mo3′ 2.820(2)
Mo1 Mo3 2.798(2)	Mo1′ Mo3′ 2.837(2)
Mo1 Mo1 3.049(3)	Mo1′ Mo1′ 3.045(3)
Mo2 Mo3 2.8138(2)	Mo2′ Mo3′ 2.8096(3)
Mo2 Mo2 2.912(4)	Mo2′ Mo2′ 2.830(4)
Mo3 Mo3 2.608(4)	Mo3′ Mo3′ 2.737(4)
Mo1 O4 2.042(12)	Mo1′ O4′ 2.035(12)
Mo1 O1 2.060(12)	Mo1′ O5′ 2.039(12)
Mo1 O5 2.068(11)	Mo1′ O1′ 2.074(12)
Mo1 O6 2.084(11)	Mo1′ O7′ 2.085(11)
Mo1 O7 2.089(11)	Mo1′ O6′ 2.093(12)
Mo2 O4 2.050(16)	Mo2′ O5′ 2.062(16)
Mo2 O5 2.069(15)	Mo2′ O4′ 2.073(15)
Mo2 O2 2.082(12) × 2	Mo2′ O2′ 2.080(12) × 2
Mo3 O6 2.033(16)	Mo3′ O6′ 2.045(17)
Mo3 O7 2.094(16)	Mo3′ O7′ 2.078(16)
Mo3 O2 2.119(12) × 2	Mo3′ O2′ 2.130(12) × 2
Lu1 O3 2.231(12) × 2	Lu1′ O3′ 2.240(12) × 2
Lu1 O1 2.282(12) × 2	Lu1′ O1′ 2.281(12) × 2
Lu1 O4 2.362(16)	Lu1′ O7′ 2.286(16)
Lu1 O2′ 2.366(12) × 2	Lu1′ O2 2.407(12) × 2
Lu2 O3′ 2.206(12) × 2	Lu2′ O3 2.216(12) × 2
Lu2 O8′ 2.256(10) × 2	Lu2′ O8 2.267(10) × 2
Lu2 O5 2.312(14)	Lu2′ O6′ 2.289(17)
Lu2 O1 2.343(12) × 2	Lu2′ O1′ 2.379(12) × 2
Lu3 O1 2.200(12) × 2	Lu3′ O1′2.178(12) × 2
Lu3 O5′ 2.207(15)	Lu3′ O3 2.240(12) × 2
Lu3 O3′ 2.244(12) × 2	Lu3′ O6 2.259(15)
Lu3 O2′ 2.609(11) × 2	Lu3′ O2 2.558(12) × 2
Lu4 O3′ 2.186(11) × 2	Lu4′ O3 2.174(12) × 2
Lu4 O8′ 2.213(10) × 2	Lu4′ O4′ 2.190(15)
Lu4 O7 2.235(16)	Lu4′ O8 2.214(10) × 2
Lu4 O2 2.649(13) × 2	Lu4′ O2′ 2.691(12) × 2

2.3. Resistivity measurements

The ac resistivity was measured on single crystals at 80 Hz with a current amplitude of 1 μA using standard four-probe techniques. Ohmic contacts to the crystals were made by attaching molten indium ultrasonically.

2.4. Magnetic susceptibility measurements

Susceptibility data were collected on cold pressed powder samples (ca. 100 mg) using a quantum design SQUID magnetometer between 4.2 and 300 K and at applied fields ranging from 0.1 to 0.4 T.

3. Results and discussion

3.1. Description of structure

The unit cell parameters of the two phases prepared here are summarized in Table 1, while relevant crystallographic data and selected bond distances from the single crystal diffraction study of $Lu_4Mo_4O_{11}$ are given in Tables 2 and 3, respectively. Fig. 1 shows the X-ray powder pattern of $Yb_4Mo_4O_{11}$ refined in profile-matching mode (Pseudo-Voigt profile function) [14]. This confirms that the phase is monoclinic although the powder and the crystals were synthesized at different temperatures. This is particularly clear for the 406 and −406 reflections, which are equivalent in the orthorhombic system and split up into two peaks in the monoclinic form (inset Fig. 1). As the monoclinic form could arise from a phase transition during the cooling process, we performed slow cooling on a powder sample of the orthorhombic compound $Tm_4Mo_4O_{11}$ and we did not observed such a transition. However, a possible phase transition $P2/m \rightarrow Pbam$ at elevated temperature is possible for the Yb and Lu compounds. The crystal structure of the monoclinic compounds $Yb_4Mo_4O_{11}$ and $Lu_4Mo_4O_{11}$ (Fig. 2) contains trans-edge-shared Mo_6 octahedral chains as previously observed in the orthorhombic form synthesized with the other rare earths (Nd to Tm). The interconnectivity between the different chains is also similar in both forms.

The lost of the *a*- and *b*-glide planes leads to two crystallographically independent molybdenum-oxide chains instead of one in the orthorhombic form. In both independent trans-edge-shared Mo_6 octahedral chains, the repeat unit, which comprises two Mo_6 octahedra, has the same $2/m$ symmetry, as previously observed in the orthorhombic form (Fig. 3). The chains also present the same type of distortion as found in the orthorhombic $R_4Mo_4O_{11}$ compounds. Indeed, we observed a pairing of the apical Mo1 and Mo1' atoms, accompanied by alternating short and long bond distances between the molybdenum atoms of the common edges. The short Mo1–Mo1 (chain 1) and Mo1′–Mo1′ (chain 2) bond distances between the apical molybdenum atoms are 2.571(3) and 2.574(3) Å in $Lu_4Mo_4O_{11}$ while the long ones

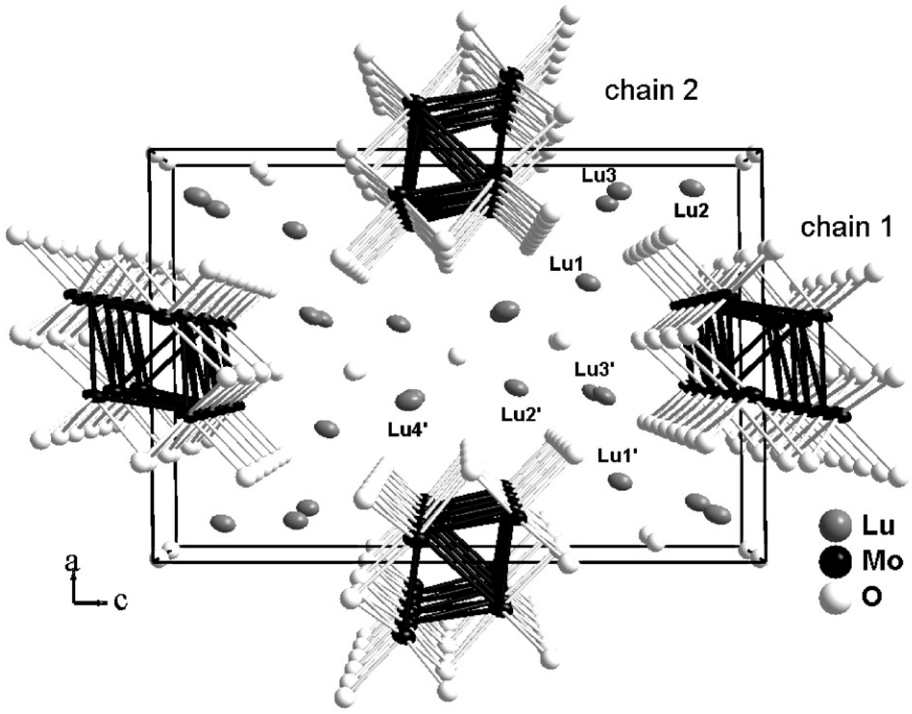

Fig. 2. The crystal structure of $Lu_4Mo_4O_{11}$ as viewed down the *b*-axis, parallel to the direction of the chain growth. Thick lines denote Mo–Mo bonding and thin lines, Mo–O and R–O bonding. Ellipsoids are drawn at the 97% probability level.

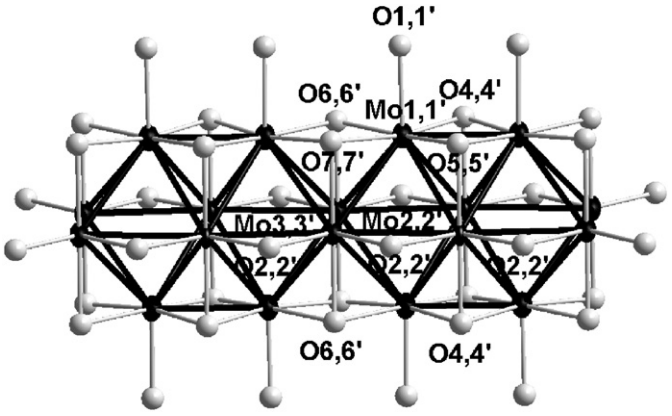

Fig. 3. A section of one molybdenum oxide cluster chain. The unprimed and primed labels are related to the chains 1 and 2, respectively. The repeat unit comprises two Mo_6 octahedra.

which are essentially nonbonding are 3.0049(3) and 3.045(3) Å [2.5689 (7), and 3.0593 (7) Å in the orthorhombic $Tm_4Mo_4O_{11}$]. The main differences between the chains 1 and 2 are observed for the short shared edges Mo3–Mo3 and Mo3′–Mo3′ which measure 2.608(4) and 2.737(4) Å in the chains 1 and 2, respectively, as well as for the longest ones Mo2–Mo2 and Mo2′–Mo2′ which are 2.912(4) and 2.830(4) Å. In the orthorhombic form, the shared-edge Mo–Mo distances are of the order of 2.60 and 2.91 Å, and thus quite comparable to those observed in the chain 1 of the monoclinic form.

The oxygen coordination of the rare earths in both the monoclinic and orthorhombic form is sevenfold and may be described as a distorted mono-face-capped trigonal prism. These sites, which share edges delimit large tunnels extending parallel to the *b*-axis where the Mo chains reside. Note that for comparison purposes, the chain axis corresponds to the *c*-axis in the orthorhombic compounds. As previously observed in the orthorhombic compounds, The Lu–O bond lengths in the Lu1, Lu1′, Lu2, and Lu2′ polyhedra range from 2.21 to 2.40 Å while they spread in a larger domain (2.20–2.69 Å) in the other polyhedra (Lu3, Lu3′, Lu4, and Lu4′) due to the fact that two bonds in each of the later four crystallographically different LuO_7 groups are significantly longer (2.61–2.69 Å) (see Table 3).

The Mo–O bond distances range from 2.033 (16) to 2.119 (12) Å and from 2.035 (12) to 2.130 (12) Å in the chains 1 and 2, respectively.

From the different Mo–O bonds, we could estimate the oxidation state of each independent molybdenum atom and, consequently, the number of electrons per Mo_4 fragment in the two independent chains in $Lu_4Mo_4O_{11}$ by using the empirical bond length–bond strength relationship developed by Brown and Wu [15] for Mo–O bonds:

$$s(\mathrm{Mo-O}) = [d(\mathrm{Mo-O})/1.882]^{-6}.$$

In the latter formula, *s*(Mo–O) is the bond strength in valence units, *d*(Mo–O) is the observed Mo–O bond distance in Å, 1.882 Å corresponds to a Mo–O single bond distance and the exponent of −6 is characteristic of the Mo atom. These calculations lead to 13.93 and 13.91 e^- per Mo_4 repeat unit in chains 1 and 2, respectively and, show that both chains behave similarly. The latter values are also in good agreement with the 14 e^- based on the

stoichiometry. Self-consistent ab initio band structure calculations carried out on the crystal structure of the orthorhombic $Y_4Mo_4O_{11}$ [6] showed that for 14 e^- a small band gap of about 0.1 eV separates the occupied band from the vacant ones. As the lowering of the crystal symmetry results in small changes on the Mo network, we could also expect a semi-conducting behavior for the monoclinic $R_4Mo_4O_{11}$ compounds.

3.2. Electrical and magnetic properties

Electrical resistivity measurements were performed on single crystals of the $Yb_4Mo_4O_{11}$ and $Lu_4Mo_4O_{11}$ compounds. The temperature dependence of the electrical resistivity measured along the chain growth shows that both compounds are semiconducting in the temperature range 100–290 K as shown by the ρ vs. T and log(ρ) vs. 1000/T plots (Fig. 4). The room temperature resistivities are 0.67 and 0.94 Ω cm and the calculated activation energies are 0.053 and 0.046 eV for the Yb and Lu compounds, respectively. These different values are similar to those reported for the orthorhombic compounds for which room temperature resistivities are comprised between 0.2 and 0.9 Ω cm and band gaps of about 0.05 eV are observed.

The temperature dependence of the molar magnetic susceptibility of $Lu_4Mo_4O_{11}$ is shown in Fig. 5. The susceptibility of the Lu compound is nearly temperature independent in the range 100–300 K with a value of about 0.9×10^{-3} emu/mol. This behavior is consistent with the absence of localized moments on the Mo atom network. The low-temperature upturn could be attributed to small amounts of paramagnetic impurities often present in the starting reactants. Fig. 6 shows the temperature dependence of the inverse susceptibility below 300 K for $Yb_4Mo_4O_{11}$. The susceptibility of $Yb_4Mo_4O_{11}$ follows the Curie–Weiss behavior at higher temperatures. The susceptibility data were fitted to a modified Curie–Weiss law,

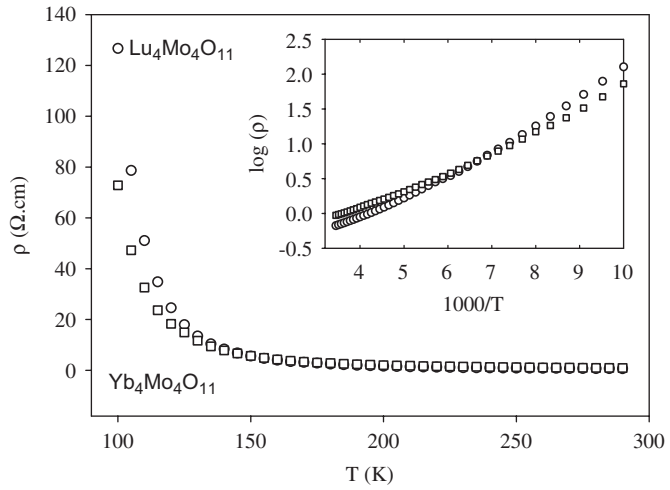

Fig. 4. Temperature dependence of the resistivity for $Yb_4Mo_4O_{11}$ (square) and $Lu_4Mo_4O_{11}$ (circle). The inset shows the Arrhenius plots.

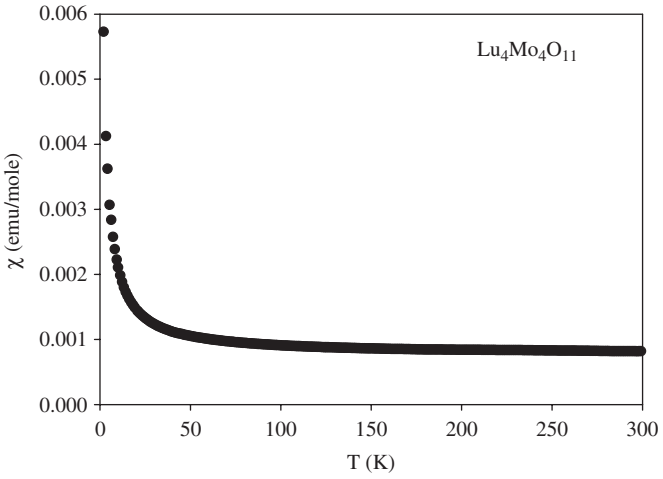

Fig. 5. Temperature dependence of the susceptibility for $Y_4Mo_4O_{11}$.

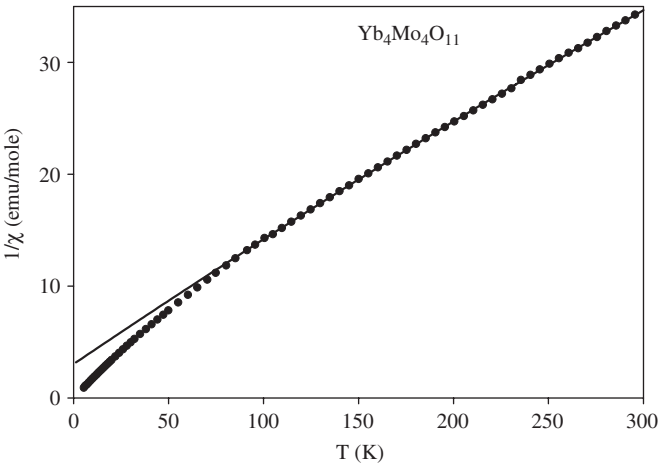

Fig. 6. Reciprocal susceptibility of $Yb_4Mo_4O_{11}$ as a function of temperature. Data were taken under an applied field of 0.4 T. The solid line represents the fit to a modified Curie–Weiss law in the range of 100–300 K.

$\chi = C/(T-\theta) + \chi_o$, in the 100–300 K temperature range with the following parameters: Weiss temperature $\theta = -40.3$ K, the temperature independent term $\chi_o = 1.12 \times 10^{-3}$ emu/mol and the Curie constant $C = 2.475$ emu K/mol. From this value of C, we can deduce an effective moment μ_{eff} equal to 4.45 μB which is very close to the value of 4.54 μB expected for trivalent Yb ions from Hund's rule. This indicates that Yb is in its 3+ magnetic valence state in $Yb_4Mo_4O_{11}$. The negative Weiss temperature indicates that the predominant exchange interactions are antiferromagnetic. No signature of magnetic ordering was found down to 1.8 K.

In summary, we have showed that the $R_4Mo_4O_{11}$ compounds with the heaviest rare earths Yb and Lu crystallize in the monoclinic space group $P2/m$ while the other members crystallize in the orthorhombic space group $Pbam$. The lowering of the symmetry, probably due to the smaller size of the rare earths, only induces small changes on the Mo network. Thus, the two independent chains have

the same MCE of 14 electrons per Mo_4 repeat unit leading to an electrical semi-conducting behavior as previously observed for the orthorhombic phases. Magnetic susceptibility measurements confirm the absence of localized moments on the Mo network and the trivalent state of the Yb cations.

References

[1] C.C. Torardi, R.E. McCarley, J. Am. Chem. Soc. 101 (1979) 3963.
[2] R.E. McCarley, Philos. Trans. R. Soc. Lond. Ser. A 308 (1982) 141.
[3] C.D. Carlson, L.F. Brough, P.A. Edwards, R.E. McCarley, J. Less-Common Met. 156 (1989) 325.
[4] K.H. Lii, R.E. McCarley, S. Kim, R.A. Jacobson, J. Solid State Chem. 64 (1986) 347.
[5] P. Gougeon, P. Gall, R.E. McCarley, Acta Crystallogr. C 47 (1991) 1585.
[6] P. Gall, N. Barrier, R. Gautier, P. Gougeon, Inorg. Chem. 41 (2002) 2879–2885.
[7] K.V. Ramanujachary, M. Greenblatt, E.B. Jones, W.H. McCarroll, J. Solid State Chem. 102 (1993) 69.
[8] T. Hughbanks, R. Hoffmann, J. Am. Chem. Soc. 105 (1983) 3528.
[9] Nonius BV, COLLECT, Data Collection Software, Nonius BV, 1999.
[10] A.J.M. Duisenberg, Reflections on area detectors, Ph.D. Thesis, Utrecht, 1998.
[11] J. de Meulenaar, H. Tompa, Acta Crystallogr. A 19 (1965) 1014–1018.
[12] A. Altomare, M.C. Burla, M. Camalli, G.L. Cascarano, C. Giacovazzo, A. Guagliardi, A.G.G. Moliterni, G. Polidori, R. Spagna, J. Appl. Crystallogr. 32 (1999) 115–119.
[13] G.M. Sheldrick, SHELXL97, Program for the Refinement of Crystal Structures, University of Göttingen, Germany, 1997.
[14] V. Petříček, M. Dušek, Jana2000—The Crystallographic Computing System, Institute of Physics, Praha, Czech Republic, 2000.
[15] I.D. Brown, K.K. Wu, Acta Crystallogr. B 32 (1976) 1957.